

Chapter

Behavior of X-Ray Analysis of Carbon Nanotubes

*Firas Habeb Abdulrazzak, Ayad Fadel Alkiam
and Falah Hasan Hussein*

Abstract

Carbon nanotubes with a variety of types occupied an amazing position compared to other nanomaterials due to rarer and specific physical and chemical properties. The behavior of graphite or graphite nanotubes theoretically and experimentally encourages their use in huge applications such as industries, fields of energy, and the environment. Many attempts are being made to get more of these benefits by a better understanding of the nature of carbon nanotubes. One of the ways to achieve this aim is by enhancing the acquaintance of characterization such as spectroscopy analysis and image microscopy. In this chapter, we are concerned with using X-ray as a source to produce clear imaginations for a tubular structure. Thus, the common ways that use X-ray as a source to interact with carbon nanotubes will be reviewed with details of characterization such as XRD, XRF, XPS, and EDX techniques.

Keywords: XRD, XRF, XPS, EDX, CNT 1

1. Introduction

The behavior of light after many years of studies and experiments opens a new orientation for science and scientists taking advantage of these features. The binary behavior of light which is represented by wave nature and particle nature enabled to appear with a variety of behaviors such diffraction, interference, and refraction. **Figure 1** shows spectrum of electromagnetic radiation which includes all the radiation types.

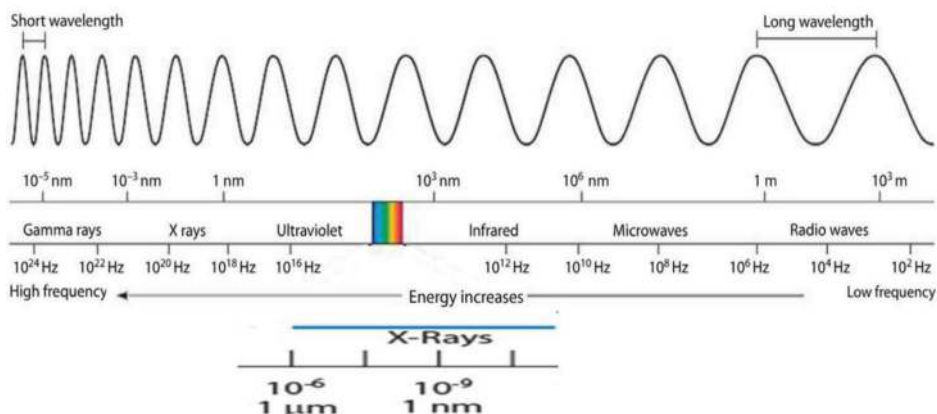


Figure 1.
The spectrum of the electromagnetic radiation with different kinds of oscillators and frequencies.

Every type in spectroscopy has specific properties which urge to use it in many applications. X-rays that are mentioned in this part with the highest-energy electromagnetic waves were commonly used in hospital and engineering applications. X-rays move in a straight line without any influence with magnetic and electric field due to the negative charge on it. In this chapter, we concern toward using X-ray behavior with materials in qualitative and quantitative applications of carbon nanotubes (CNTs).

2. Carbon nanotubes (CNTs)

The term carbon nanotubes (CNTs) refers to nanomaterials with a tubular structure consisting of carbon atoms only bonded with each other by sp^2 hybridization. The talks about CNTs were increasing 27 years ago after Lijima reported the first clear research [1], which represents the starting point of the huge attention on CNTs. The attentions appeared as reported literature deals with synthesis, purification, characterization, and studding physiochemical properties [2, 3]. Many results were paving the way for many successful attempts to use CNTs practically in many fields of science. The applications such as energy, construction, treatment, and environmental protection fields [4] were enhancing to increase the attention to make more clear images for CNTs. Carbon nanotubes (CNTs) were synthesized by chemical vapor deposition CVD, arc-discharge ADs, laser ablation LAs [4], and flame method FM [5]. Many types of apparatus were used to identify CNTs such scanning electron microscopy (SEM), transmission electron microscopy (TEM), helium ion microscopy (HIM), Raman microscopy, and X-ray family. In this chapter, we focus on the characterization of carbon nanotubes by using a specific technique that is used for this purpose, which depends on X-ray as a source to show the carbonic composition. The orientation of atoms within the lattice determines the peak intensity. Therefore, the X-ray behavior with materials is the fingerprint for periodic atomic arrangements in a known material. The start point with these aims to classify CNTs into two types depending on the number of sheets as shown in **Figure 2**.

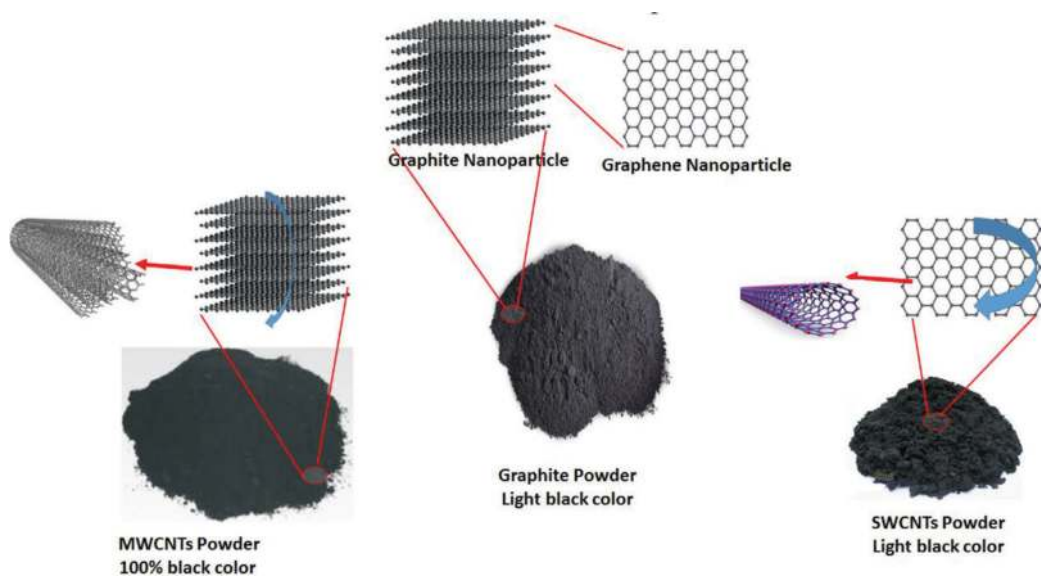


Figure 2.
Figure shows the classification of CNTs by the number of sheets.

2.1 Graphite nanotubes (GNTs)

The graphite nanotubes refer to graphite materials that show a tubular structure with nanometer dimensions, which are commonly known as multi-walled carbon nanotubes (MWCNTs).

2.2 Graphene nanotubes (gNTs)

The second type refers to graphite structure which forms nanotubes and that includes three types:

2.2.1 Single walled carbon nanotubes (SWCNTs)

There is one sheet of carbon atoms that forms SWCNTs, characterized by diameter 0.5–1.5 nm [6].

2.2.2 Double walled carbon nanotubes (DWCNTs)

Two sheets of carbon atoms are flopped with each other to form DWCNTs, with 2.4–3.2 nm diameter [7].

2.3 Few walled carbon nanotubes (FWCNTs)

When the number of sheets is 2–6, the type is known as few walled carbon nanotubes FWCNTs. The diameter as we mentioned before was decided by the number of sheets that forms it, which ranges between 4 and 9 nm [8].

3. How X-ray is produced?

X-rays are generated in an X-ray tube responsible to generate X-rays when an electron beam is passed between a cathode part and an anode. **Figure 3** includes the essential components for an X-ray system when a stream of fast-moving accelerated electrons is transferred from the cathode to the anode. The interaction of electrons with atoms produces a great amount of energy [9] equal to 1% of the total energy while 99% appear as heat when removed from the anode. When current is passed through a conductive material, the material will heat due to the resistance in the

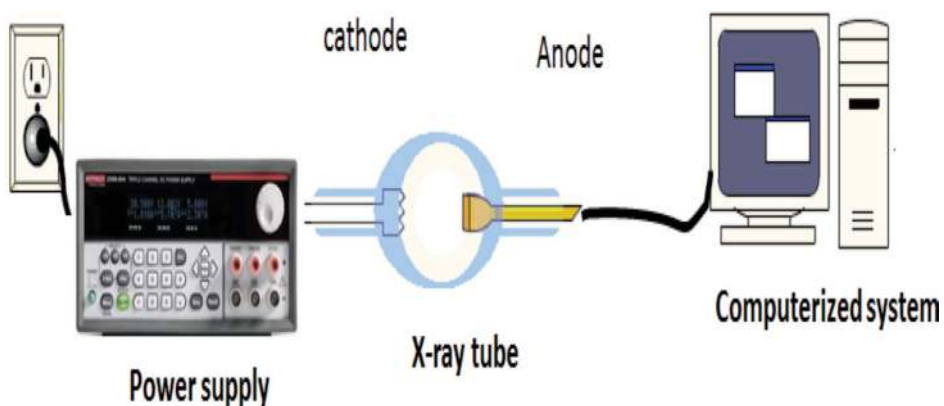


Figure 3.
Figure for essential components of X-ray generator.

wire causing excitation of the electrons and energy expansion. When the energy of the electron expands, it will return to the wire to become heat again and becomes a source of electrons [10]. The positive charge and negative charge will form a strong, attractive force to accelerate the electrons, which could increase the forces of X-ray by increasing the voltage applied to the anode.

4. Debye-Scherrer equation and Bragg's law

The X-rays are commonly generated by a cathode ray tube, occupied with a specific filter to form monochromatic radiation, which concentrates toward the sample. **Figure 4** represents Bragg's law ($n\lambda = 2d \sin \theta$) referring to the specific case of diffraction, which depends on the angles of scattering (θ) coherent and incoherent monochromatic light (λ) from a crystal lattice consisting of n sheets. This equation ($d = (K*\lambda)/(\beta*\cos \theta)$) is commonly used to find partial size (d) for materials [11] when the benefit from the behavior of incident and monochromatic light (λ) with specific angle (θ) is decided from the nature of the construction material. The value of (d) was calculated for the line broadening at half the maximum intensity ($\beta = \text{FWHM}$), while the shape factor (K) was typically equal to about 0.9, which changes with shape of the crystallite. When X-rays are incident on an atom, they make the electronic cloud move, as does any electromagnetic wave. The movement of these charges radiate wave with the same frequency, blurred slightly due to [10] a variety of effects, and this phenomenon is known as Rayleigh scattering (or elastic scattering). The scattered waves can themselves be scattered, but this secondary scattering is negligible.

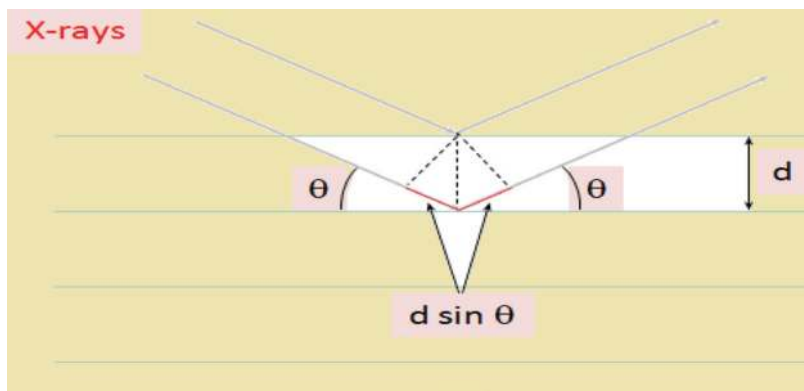


Figure 4.
The typical equation to characterize the structure of the crystal.

5. X-ray diffraction analysis (XRD)

XRD analysis is a unique method to find qualitative properties such as crystallinity, types, fingerprints, and quantitative material [11]. Graphite and graphene show great similarity in XRD with GNTs and joints, respectively, for the main peaks [12–14] at ≈ 24 and 43° . Most references shows these two peaks high degree of similarity, especially at the first strong peak. **Figure 5** shows the two peaks: the first on the left is of very high intensity with less width compared with the second peak at the right. The length and width of the peaks were commonly used to recognize the nature of crystal size. Generally, for carbon nanotubes, the first peak at the right refers to crystalline or amorphous nature; thus, the width increases with reducing intensity or length, which refers to exist in amorphous crystal form [15].

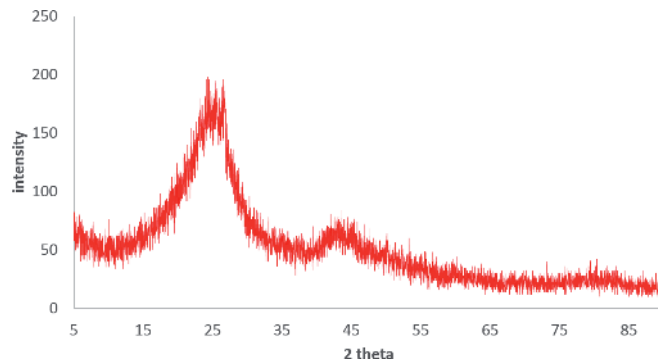


Figure 5.
Typical XRD analysis for CNTs.

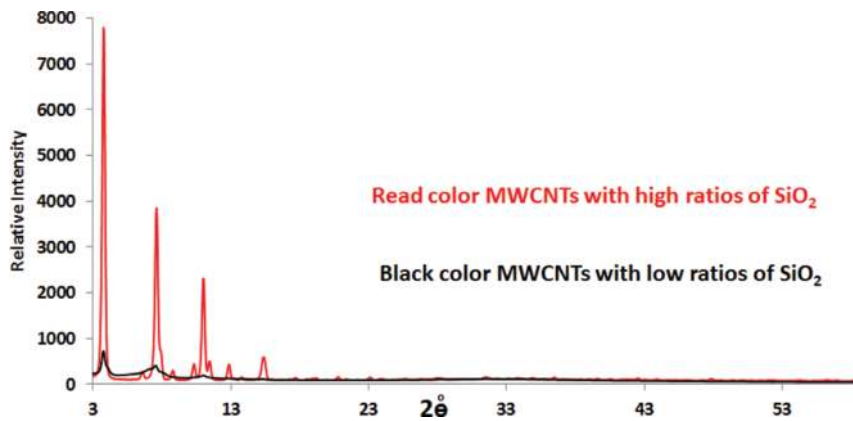


Figure 6.
XRD patterns for synthesized MWCNTs with high and low ratios of SiO_2 .

Typically, the impurities influence Directly on the position of two peaks due to low intensity of the peaks compared with the impurities. For example, MWCNTs were prepared by chemical vapor deposition using 1-propanol as a source of carbon at 700°C on the surface of silica as support for precipitation as shown in **Figure 6**. The XRD analysis of synthesized MWCNTs is reported in **Figure 6**, showing the effect of amorphous carbon and Si, Na, Fe, and Mg in the diagram of XRD which removed or at least limited the appearance of the two characterized peaks of CNTs. The elements which were mentioned causing a disappearance [16] for the carbon tubular structure had spread between these components. Thus, XRD for the sample was disappearing due to the higher intensity of many crystal structures [17] of the element when reached 8000 units compared with low intensity of carbon with less than 120 units.

Figure 7 shows two notes to be taken care of when using XRD to predict the existence of CNTs: the first, the impurities inevitably caused shift for the two peaks due to real connection between tubular structure and impurities. The second refers to influence of interference, which causes removal of the second peak or complete disappearance due to the high difference between importers and carbon material. The last two points look like a photograph; picture was taken for wood including very high Trees compared to grass and few small herbs, the result or the image should be favored the trees.

The typical peak at $\approx 26.0^\circ$ represents the characteristic graphitic peak [18] arising due to the tubular structure of the carbon atoms in the sample with (002) planes. This peak shifted to more than 28.8° , which affects [19] the ratios of impurities in the sample. The typical peaks near 43.2 and 53.74° disappeared due to

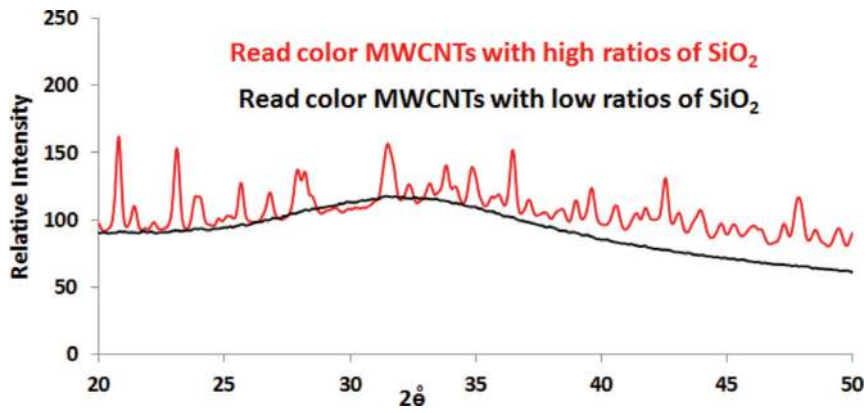


Figure 7.
XRD patterns for synthesized MWCNTs with high and low ratios of SiO₂ from 20 to 50°.

existing Si and Fe [19], which show strong peaks at ≈ 42 and 52° , respectively, when interfering with the weak peaks of CNTs.

5.1 MWCNTs vs. SWCNTs

This part represents one of the most important section for the science of nanomaterials generally and nanotubes particularly, which could be dependent on to identification and discrimination between SWCNTs, DWCNTs, FWCNTs, and MWCNTs. The interest in this part refers to direct application for the two roles of diffraction and the number of sheets that form the skeleton of tubular structures. This fact we referred to in the International Conference on Chemistry and Applied Research in October 29–30, 2018 Prague, Czech Republic. The fact was that there were many noises for SWCNTs as compared with MWCNTs with the two peaks, which enhance forming the noises to reduce the number of graphene sheets, as following arrangement for CNT types. Thus, the ratios of noise can be arranged as follows:

$$\text{SWCNT} > \text{DWCNT} > \text{FWCNT} > \text{MWCNT}$$

Figure 8 explains the behavior of CNTs when an increase in the number of inner shells causes more intensity for the peaks with MWCNTs than SWCNTs which show in pure and with mixture of composite. This fact was in agreement with a good

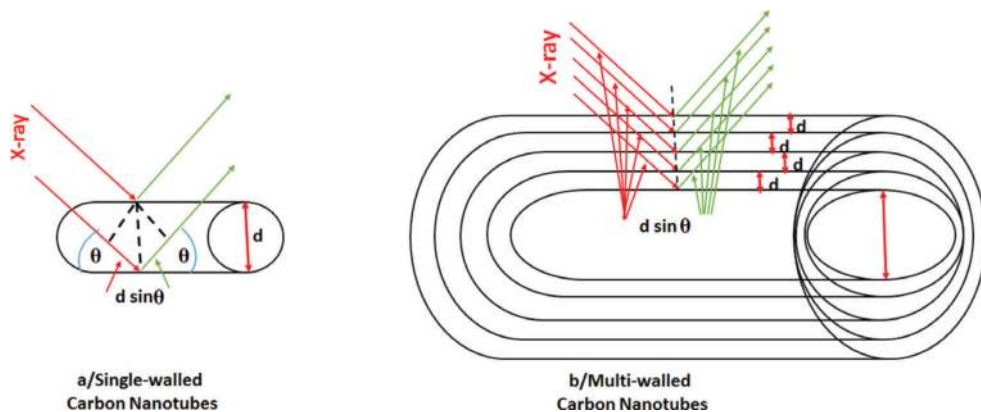


Figure 8.
Figure shows the influence of number of layers with X-ray diffraction.

deal of experimental research, such as studies by Mhamane et al., Tang et al., and Chang et al. [20–22] for graphite and graphene, showing noise with graphene and graphene oxide while reduced noise with graphite.

6. X-ray fluorescence (XRF)

The principles of this technique depend on removing the electron from lower energy level, causing an unstable state for atoms; therefore, the electron in the higher energy shell moves inside the atom. The value of the difference between higher and lower levels was emitting as specific energy to identify the fluorescing element and is proportional to the amount of element. Generally, the characteristic peaks are labeled X-rays as K, L, M, and N refer to the shells they activated or (α),

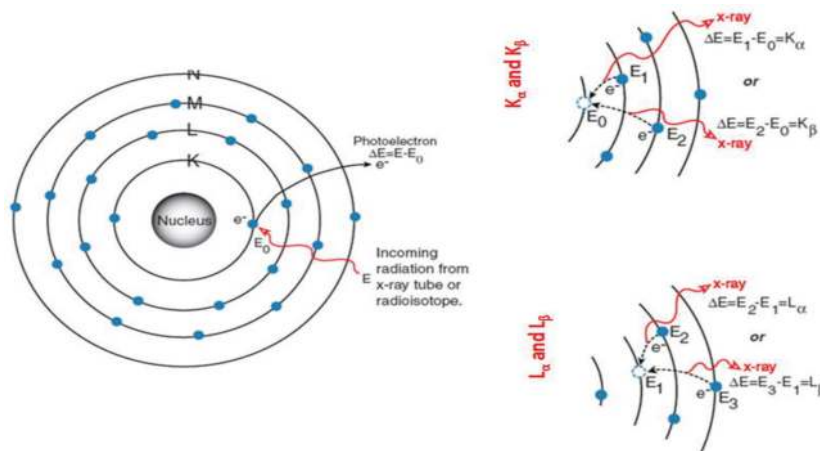


Figure 9.
 A supposed mechanism for forming X-ray radiation.

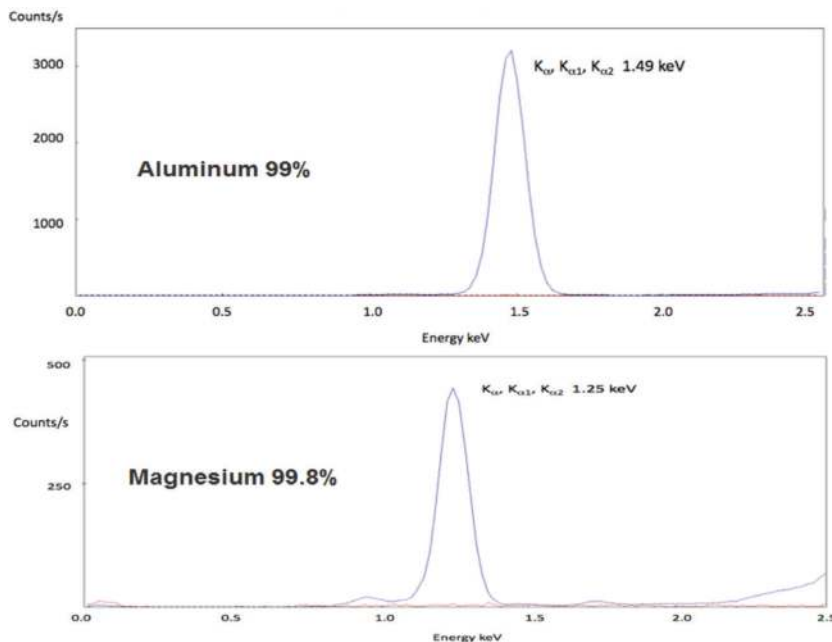


Figure 10.
 XRF spectrum for aluminum and magnesium that are mostly used as a catalyst for growth of CNTs.

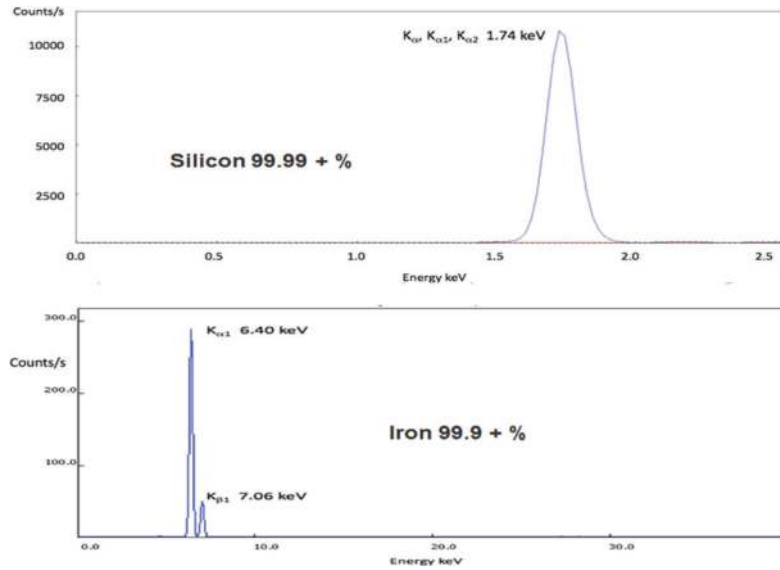


Figure 11. XRF spectrum for silicon and iron that are mostly used as a support for catalyst CNTs.

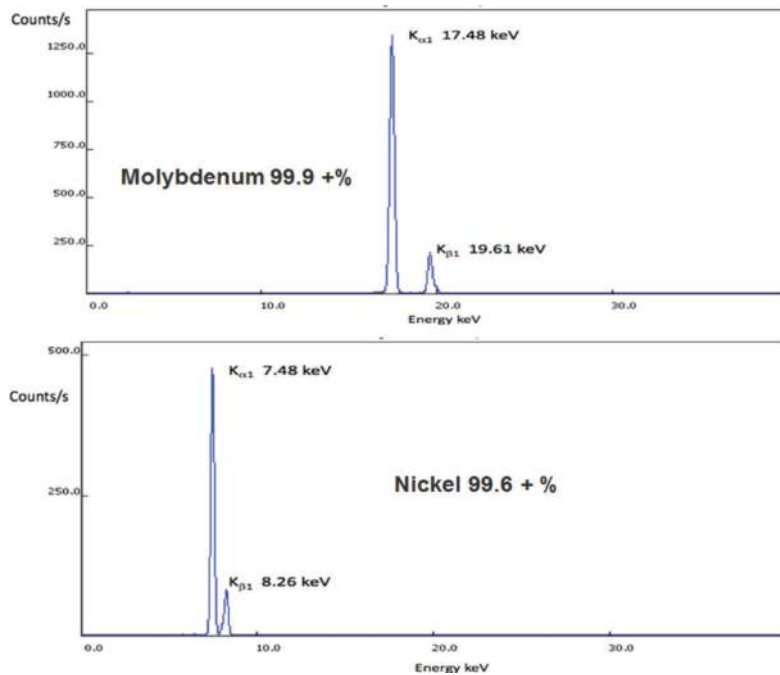


Figure 12. XRF spectrum for nickel and molybdenum used as a catalyst for growth of CNTs.

(β), and (γ) depend on the transitions of electrons from higher shells. However, $K\alpha 2$ means the transition of an electron from the L to the K shell, while $K\beta 1$ represents the transition of an electron from the M to the K shell of multiple orbits.

Figure 9 refers to the behavior of elementary information that makes possibilities to quantify identification of metals, which are commonly used as a catalyst for precipitation of carbon on the support of the catalyst to form CNTs. The advantage of this technique is that it is rapid and it is easy to treat the sample without any complications and without being affected by chemical bonding. The disadvantages include limited abilities to identify trace contents in addition to the high radiation that may cause damage for tubular structure CNTs. Singhal et al. [23] reported the qualitative

analysis when analyzing CNT-coated Al. The analysis showed three peaks at 2θ which are 32.5 , 50.8 , and 144.7° corresponding to C $K\alpha$, O $K\alpha$, and Al $K\alpha$ spectral lines, respectively, related to the presence of C, O, and Al elements in the composite. The quantitative analysis for synthesized composite confirms that the percentage weight of C, which corresponds to CNTs, was 3.95%. XRF can be used for studied catalyst content in CNTs during the steps of purification, but in the same time, it cannot be used to determine amorphous carbon content. [24]. **Figures 10–12** show aluminum, magnesium, silicon, iron, molybdenum, and nickel that are commonly used for synthesized carbon nanotubes as a catalyst or support for precipitation.

7. Energy-dispersive X-ray spectroscopy (EDX)

The energy dispersive X-ray analysis EDX and EDA sometimes EDS or energy dispersive X-ray Microanalysis EDXMA. This technical method depends on the interaction of X-ray radiation with a sample when convert to single that refers to the material in the chemical area and thus is used for elemental characterization. The efficiency for characterization can be related to the fundamental principle that each element has a unique atomic structure allowing a unique set of peaks in its electromagnetic emission spectrum [10]. Mostly, scanning electron microscopy (SEM) supplied with EDX is used to qualitatively and quantitatively analyze the elements present in the selected area of the SEM image to estimate of CNTs' metal contents and impurities. Together, the SEM and EDX capabilities allow irradiation by a focused electron beam, imaging secondary or back-scattered electrons and an energy analysis of X-rays. Typical SEM applications include plan view and cross-sectional imaging for process development and failure analysis. EDX applications include specific defect analysis or composition analysis. **Figures 13 and 14** refer to EDX analysis for SWCNTs and MWCNTs made from Aldrich by chemical vapor deposition with high purities. When using this technique should, analysis of large-scale CNTs should be avoided since it may cause error in identification due to overlap of peaks for CNTs with many elements such as Ti $K\beta$, Mn $K\beta$, and Fe $K\alpha$ [25].

Figure 15 shows an EDX spectrum of MWCNTs synthesized by the CVD technique from decomposition date palm seeds at 700°C on the boat of silicon as supported for Mo, which was used to grow MWCNTs. The spectrum shows four strong peaks, which represent carbon, silicon, Al, and Mo. The C refers to carbon materials, which mostly refer to the growth of CNTs on Mo that covers the surface of

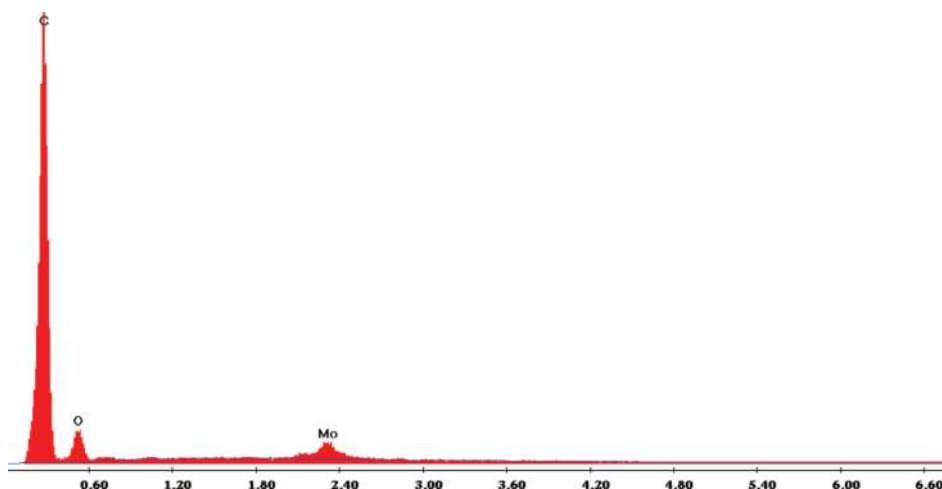


Figure 13.
EDX spectrum for Aldrich SWCNTs which were synthesized by the CVD method.

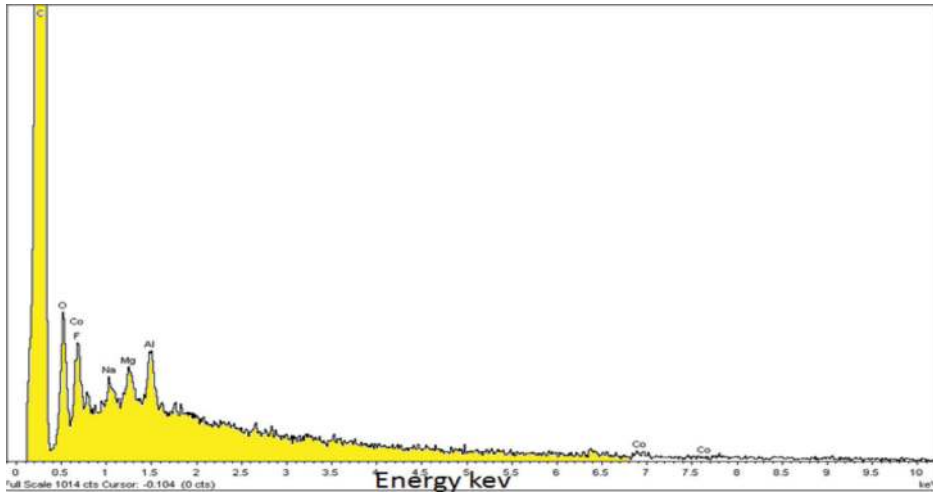


Figure 14.
EDX spectrum for Aldrich MWCNTs which were synthesized by the CVD method.

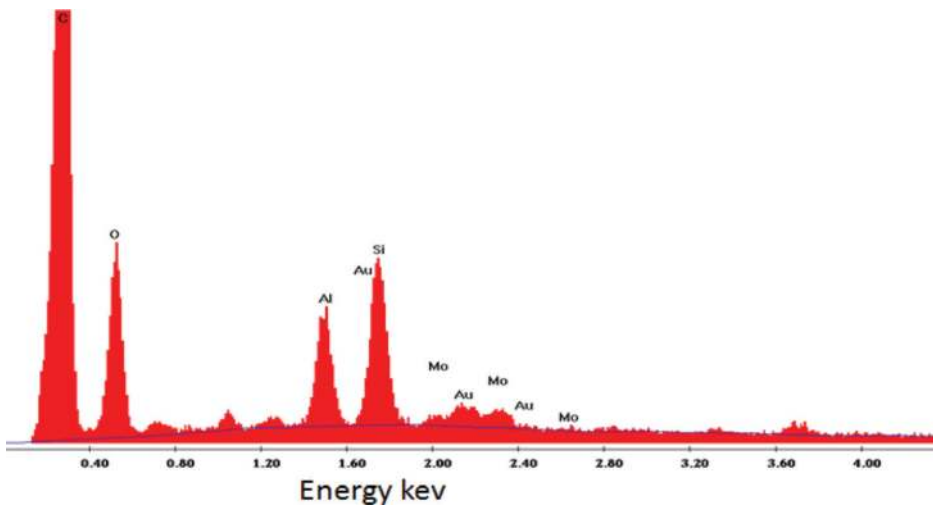


Figure 15.
EDX spectrum for Aldrich MWCNTs which were synthesized by the CVD method.

the silica boat. The O refers to the groups of oxide which are produced by a purification process by using nitric acid (5 M). **Figure 16:** EDX spectrum for MWCNTs synthesized by CVDs from decomposition date palm seeds at 700°C on the boat of silica as supported for Mo, which used to growth CNTs Shows an EDX spectrum of us received MWCNTs when synthesized from propanol at 700°C by CVDs with used silica as support and iron oxide as catalyst for growth CNTs. The EDXs in **Figure 16**, with three strong peaks, represent silicon, and two for Fe. This indicates that the growth of CNTs originated from Fe or Fe carbide particles on the silicon substrate. The peak of C is short, which refers to low precipitation on the surfaces of the boat.

The most important thing when used EDX represented by the area which needs to make quantitative and qualitative analysis due to heterogeneous distribution of the elements in analyzing samples. We mention before the aims from analysis whom responsible to decide the area of analysis. 9. X-ray photoelectron spectroscopy (XPS) is a quantitative technique that deals with measures, empirical formula, and chemical and electronic state with elemental composition in high sensitivity that exists within a material [10]. The most important nature of XPS is that it shows not only qualities of elements starting from lithium and above but also the nature of

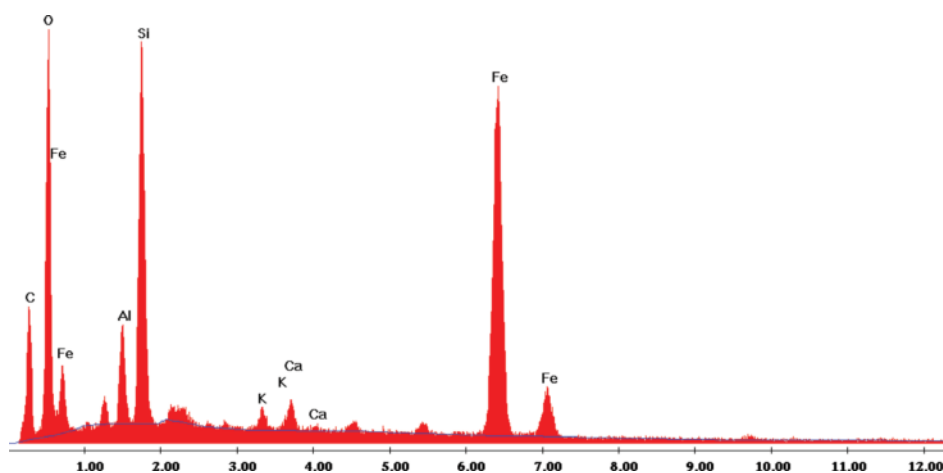


Figure 16.
EDX spectrum for MWCNTs prepared from propanol at 700°C by CVD with silica used as a support and iron oxide as a catalyst.

local bonds for all the components in a mixture. XPS spectra are obtained by irradiating thickness of analyzing material, arranged between 0 and 10 mm with a beam of X-rays to measure the number and energy of escaped electrons in high vacuum ambience. It mostly requires large amounts of sample to reach 5 mg to produce ideal analysis that commonly produces ambiguous and interpreted peaks, which are simplified by a specific computerized system. The XPS spectrum is represented by plotting the binding energy (eV) between different atoms with intensity of energy in the chemical environment of materials. The ideal detection limits for most of the elements are in the parts per thousand range while parts per million (ppm) could be made when special needs were provided such as concentration on the top surface and very long collection time. The oxidation state represents the main criterion for identifying [26–29] the elements due to influence with the local bonding environment for the atoms in molecules. In the case of carbon nanotubes, the binding energy of C1s electron is 284.6 eV; when binding with other atoms, it will be chemically shifted, which depends on the chemical state of neighboring atoms. For example, the carbon in the polymer structure shows increasing binding energy as follows [26–31]:

Carbide ($-C_2-$) < Silicone ($-Si-CH_3$) < Methylene/Methyl/Hydrocarbon ($-CH_2-CH_2-$ < CH_3-CH_2- < $-CH=CH-$) < Amine ($-CH_2-NH_2$) < Alcohol ($-C-OH$) < Ketone ($-C=O$) < Organic Ester ($-COOR$)

The characterization peak of carbon nanotubes corresponding to C=C for graphene layer for spectra at about 284 eV.

For example, the synthesized carbon nanotubes from natural petroleum gas were tested with X-ray photoelectron spectroscopy. The nature of different groups that were covalently linked to the nanotube surface is reported in **Table 1**, where existence of C=C refers to nanotubes or graphene sheets. To have a more clear and more specific explanation, we review different groups that are covalently linked to the nanotube surface to improve C=C which refers to nanotubes by XPS analysis. The carbon nanotubes (MWCNTs) were synthesized by the chemical flame deposition method by using liquefied petroleum gas as a source of carbon on the surface of iron as supported for precipitation at 180°C. **Figure 17** shows the photoemission C1s peaks that were studied between 282 and 292 eV. A dominant peak is observed at 284 or 285 eV of the sp^2 hybridized C=C bonds in extensive conjugated systems

Functional Group		Binding Energy (eV)
hydrocarbon	$\underline{\text{C}}\text{-H}$, $\underline{\text{C}}\text{-C}$	285.0
amine	$\underline{\text{C}}\text{-N}$	286.0
alcohol, ether	$\underline{\text{C}}\text{-O-H}$, $\underline{\text{C}}\text{-O-C}$	286.5
Cl bound to C	$\underline{\text{C}}\text{-Cl}$	286.5
F bound to C	$\underline{\text{C}}\text{-F}$	287.8
carbonyl	$\underline{\text{C}}\text{=O}$	288.0

Table 1.
Common values of band that predicted existence in CNTs.

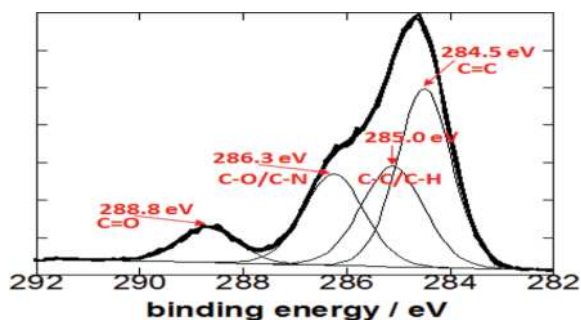


Figure 17.
XPS C 1s spectra of synthesized MWCNT between 282 and 292 eV. Arrows show possible positions of carbon peaks.

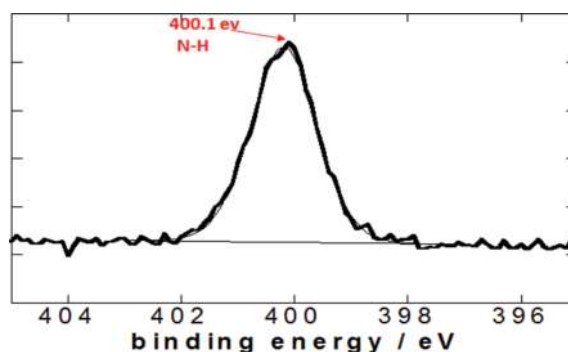


Figure 18.
XPS of N–H spectra between 396 and 404 eV. Arrows show possible position of the N–H peak.

[26, 27], which mostly refers to graphene sheets in carbon nanotubes. The same figure includes a peak at 285.0 eV, which is characteristic of sp³ hybridized C–C bonds present at defective locations [28] and tubular structure asymmetry related to C–H and C–C [29]. Two other photoemission peaks are observed at 286.3 and 288.8 eV. The first peak at 286.3 eV is attributed to carbon atoms bonded to oxygen atoms C–O which bonded with C–N. The second peak at 288.8 eV is characteristic of carbon atoms of carbonyl groups (C=O) [30]. **Figure 18** shows N 1s 400.1 eV spectra, which refer to N–H related to N–C=C groups [31].

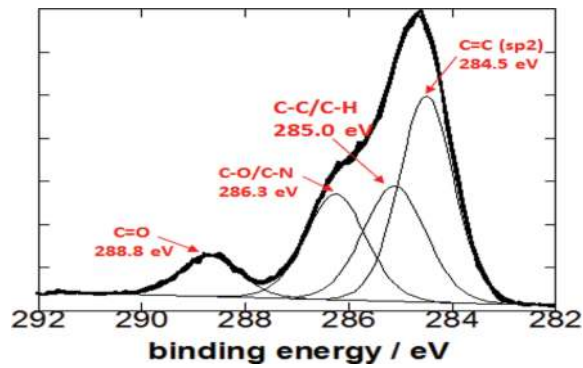


Figure 19.
XPS C 1s spectra of synthesized MWNT between 282 and 292 eV. Arrows show possible positions of carbon peaks.

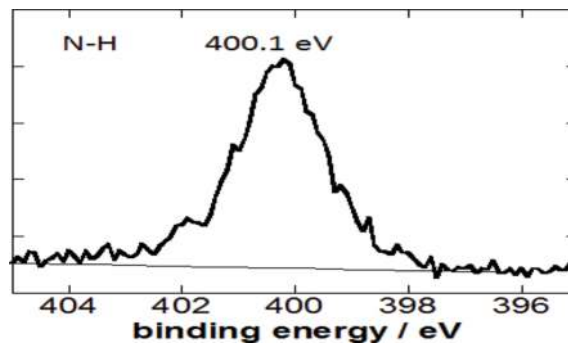


Figure 20.
XPS of N-H spectra between 396 and 404 eV.

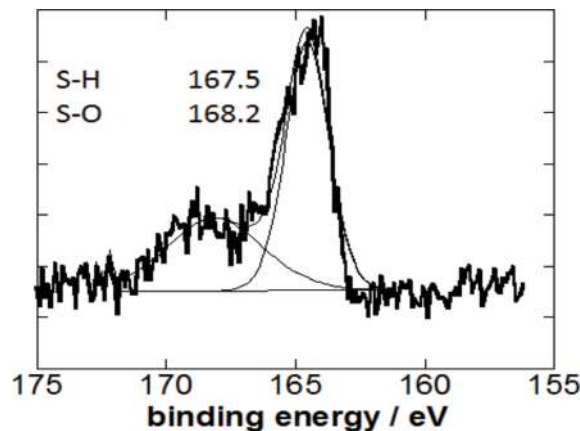


Figure 21.
XPS of S spectra between 155 and 175 eV.

Figure 19 shows the XPS spectra of the second sample with different peaks at 284.5, 285.0, 286.3, and 288.8 eV. The first peak at 284.5 eV corresponds to C=C for graphene sheets [32] while the neighboring peak at 285.0 eV corresponds to C-C and C-H. The second peak at 286.3 eV is related to C-O/C-N [33]. The third peak at 288.8 eV corresponds to C=O [30]. **Figure 20** shows the N 1s spectra at 400.1 eV, which refers to N-H related to N-C=C groups [31].

Figure 21 refers to two overlapping peaks together at 167.5 and 168.2 eV, which correspond to S-H and S-O, respectively, while the strong peak at 164.7 eV sp² indicates the S-C bond [34]. The second sample shows an existence of sulfur which can be related to the oil that was used to prepare this sample only.

8. Conclusion

Many techniques and methods are commonly used for characterizing and analyzing nanomaterials such as SEM, TEM, HIM, Raman microscopy, UV-visible reflection, and X-ray family. All of the techniques mentioned before and others depend on reactant materials with electrons. X-ray led to many ways of getting huge information about the composition of materials and the nature of construction. X-ray family is supplied mostly, nondestructively and fast, with the ability to provide the basic structural information that is essential for identification. In our chapter, X-ray families were used for quantification and qualification of carbon nanotubes. XRD, XRF, EDX, and XPS were used in this chapter with many synthesized CNTs to show the abilities for evaluating the purities which are very important in applications. We anticipate that the results of this study will help to offer guidelines for understand CNTs structures by X-ray family to increase the probabilities for benefit from CNTs.

Author details

Firas Habeb Abdulrazzak^{1*}, Ayad Fadel Alkiam² and Falah Hasan Hussein^{3,4}

1 Department of Chemistry, College of Education for Pure Science, Diyala University, Diyala, Iraq


2 Department of Chemistry, College of Science, Babylon University, Hilla, Iraq

3 Department of Pharmaceutics, College of Pharmacy, Babylon University, Hilla, Iraq

4 Department of Research and Studies, Al-Mustaqbal University College, Babylon, Iraq

*Address all correspondence to: firmas_habeb2000@yahoo.com

IntechOpen

© 2019 The Author(s). Licensee IntechOpen. This chapter is distributed under the terms of the Creative Commons Attribution License (<http://creativecommons.org/licenses/by/3.0>), which permits unrestricted use, distribution, and reproduction in any medium, provided the original work is properly cited. 

References

- [1] Iijima S. Helical microtubules of graphitic carbon. *Nature*. 1991;**354**:56-58
- [2] Popov V. Carbon nanotubes: Properties and application. *Materials Science and Engineering R*. 2004;**43**(3):61-102
- [3] Yadav B, Kumar R. Structure, properties, and applications of fullerenes. *International Journal of Nanotechnology and Applications*. 2008;**2**(1):15-24
- [4] Falah HH, Firas HA, Ayad FA. *Nanomaterials: Biomedical and Environmental Applications*, Chapter 1, 4: *Nanomaterials: Synthesis and Characterization*. 1st ed. Wiley; 2018
- [5] Firas HA, Ahmad MA, Falah HH. Synthesis of multi-walled carbon nanotubes from Iraqi natural gas/CO mixture by catalytic flame fragments deposition method. *Asian Journal of Chemistry*. 2019;**31**(1):247-250
- [6] Bansi D, Saurabh S, Shine A. Biosensors for food toxin detection: Carbon nanotubes and graphene. In: *Materials Research Society Symposium Proceedings 1725*. Materials Research Society; 2015
- [7] Jaehyeok D, Jongsoo L. Prediction of the mechanical behavior of double walled-CNTs using a molecular mechanics-based finite element method: Effects of chirality. *Computers and Structures*. 2016;**169**:91-100
- [8] Elsa G, Casanova O, Román M, Aguilar A, Espinosa F. Synthesis of carbon nanotubes of few walls using aliphatic alcohols as a carbon source. *Materials*. 2013;**6**(6):2534-2542
- [9] Skinner CH. Review of soft X-ray lasers and their applications. *Physics of Fluids B: Plasma Physics*. 1991;**3**:2420-2430
- [10] Yoon TH. Applications of soft X-ray spectromicroscopy in material and environmental sciences. *Journal Applied Spectroscopy Reviews*. 2009;**44**(2):91-122
- [11] Ahmad M, Foroughi MR, Monish MR. Modified Scherer equation to estimate more accurately nano-crystallite size using XRD. *World Journal of Nano Science and Engineering*. 2012;**2**:154-160
- [12] Rasel D, Abd Hamid SB, Ali ME, Seeram R, Wu Y. Carbon nanotubes characterization by X-ray powder diffraction—A review. *Current Nanoscience*. 2015;**11**:23-35
- [13] Li ZQ, Lu CJ, Xia ZP, Luo ZZ. X-ray diffraction patterns of graphite and turbostratic carbon. *Carbon*. 2007;**45**(8):1686-1695
- [14] Johra FT, Lee J-W, Jung W-G. Facile and safe graphene preparation on solution based platform. *Journal of Industrial and Engineering Chemistry*. 2014;**20**:2883-2887
- [15] Longlong X, Yifu Z, Xiongzhi Z, Yu H, Xiaoyu T, Chi H, et al. Designed synthesis of tunable amorphous carbon nanotubes (a-CNTs) by a novel route and their oxidation resistance properties. *Bulletin of Materials Science*. 2014;**37**(6):1397-1402
- [16] Tam NT, Nghia NX, Khoi PH, Minh PN. Analyzing the purity of carbon nanotubes by using different methods. *Journal of the Korean Physical Society*. 2008;**52**(5):1382-1385
- [17] Chen XH, Chen CS, Chen Q, Cheng FG, Zhang G, Chen ZZ. Non-destructive purification of multi-walled carbon nanotubes produced by catalyzed CVD. *Materials Letters*. 2002;**57**(3):734-738
- [18] Nishimura K, Okazaki N, Pan L, Nakayama Y. In situ study of iron catalysts

- for carbon nanotube growth using X-ray diffraction analysis. *Japanese Journal of Applied Physics*. 2004;**43**(4A):471-474
- [19] Andrew R, Jacques D, Qian D, Dickey EC. Purification and structural annealing of multi walled carbon nanotubes at graphitization temperatures. *Carbon*. 2001;**39**(11):1681-1687
- [20] Mhamane KD, Ramadan W, Fawzy M, Abhimanyu R, Megha D, Chandra R, et al. From graphite oxide to highly water dispersible functionalized graphene by single step plant extract-induced deoxygenation. *Green Chemistry*. 2011;**13**:1990-1996
- [21] Yu FT, Fuqiang H, Wei Z, Liu Z, Wan D. Synthesis of graphene-supported $\text{Li}_4\text{Ti}_5\text{O}_{12}$ nanosheets for high rate battery application. *Journal of Materials Chemistry*. 2012;**22**:11257-11260
- [22] Leea CY, Baeb J-H, Kim T-Y, Chang S-H, Kim SY. Using silane-functionalized graphene oxides for enhancing the interfacial bonding strength of carbon/epoxy composites. *Composites Part A: Applied Science and Manufacturing*. 2015;**75**:11-17
- [23] Singhal SK, Seth RK, Satish T, Rajeev C, Mathur RB. Synthesis and characterization of carbon nanotubes over iron carbide nanoparticles coated Al powder using thermal chemical vapor deposition. *Applied Nanoscience*. 2013;**3**:41-48
- [24] Brandon C, Joshua H, Joe V, Williams S. X-ray fluorescence as a method of monitoring metal catalyst content during the purification of carbon nanotubes. *Radiation Physics and Chemistry*. 2012;**81**(2):131-134
- [25] Goldstein J, Newbury DE, Joy DC, Lyman CE, Echlin P, Lifshin E, et al. *Scanning Electron Microscopy and X-ray Microanalysis*. Berlin: Springer; 2003
- [26] Yang DQ, Rochett JF, Sacher E. Controlled chemical functionalization of multiwalled carbon nanotubes by kiloelectronvolt argon ion treatment and air exposure. *Langmuir*. 2005;**21**(18):8539-8545
- [27] Li M, Boggs M, Beebe TP, Huang CP. Oxidation of single walled carbon nanotubes in dilute aqueous solutions by ozone as affected by ultrasound. *Carbon*. 2008;**46**:466-475
- [28] Ramana GV, Kumar RN, Prabhakar KVP, Jain PK, Balaji P. Mechanical properties of multi-walled carbon nanotubes reinforced polymer. *Indian Journal of Engineering and Materials Science*. 2010;**17**(5):331-337
- [29] Dilip CD, Veena S. Analysis of carbon nanotubes produced by pyrolysis of composite film of poly (vinyl alcohol) and modified fly ash. *Materials Sciences and Applications*. 2012;**3**:103-109
- [30] Xia W, Wang Y, Bergstraszer R, Kundu S, Muhler M. High-density and well-aligned carbon nanotubes formed by surface decomposition of SiC. *Applied Surface Science*. 2007;**254**:257-261
- [31] Yang K, Gu M, Guo Y, Pan X, Mu G. Effects of carbon nanotube functionalization on the mechanical and thermal properties of epoxy composites. *Carbon*. 2009;**47**:1723-1737
- [32] Shuai W, Tang LA, Qiaoliang B, Ming L, Goh SDBM, Loh KP. Room-temperature synthesis of soluble carbon nanotubes by the sonication of graphene oxide nanosheets. *Journal of the American Chemical Society*. 2009;**131**(46):16832-16837
- [33] Silva WM, Hélio R, Seara LM, Calado HDR, Ferlauto AS, Paniago RM, et al. Surface properties of oxidized and aminated multi-walled carbon nanotubes. *Journal of the Brazilian Chemical Society*. 2012;**23**(6):1078-1086
- [34] Samarendra ND, Dulal D, David CF. Study of sulphur in Assam coals by X-ray photoelectron spectroscopy. *Fuel*. 1983;**62**(7):840-841